

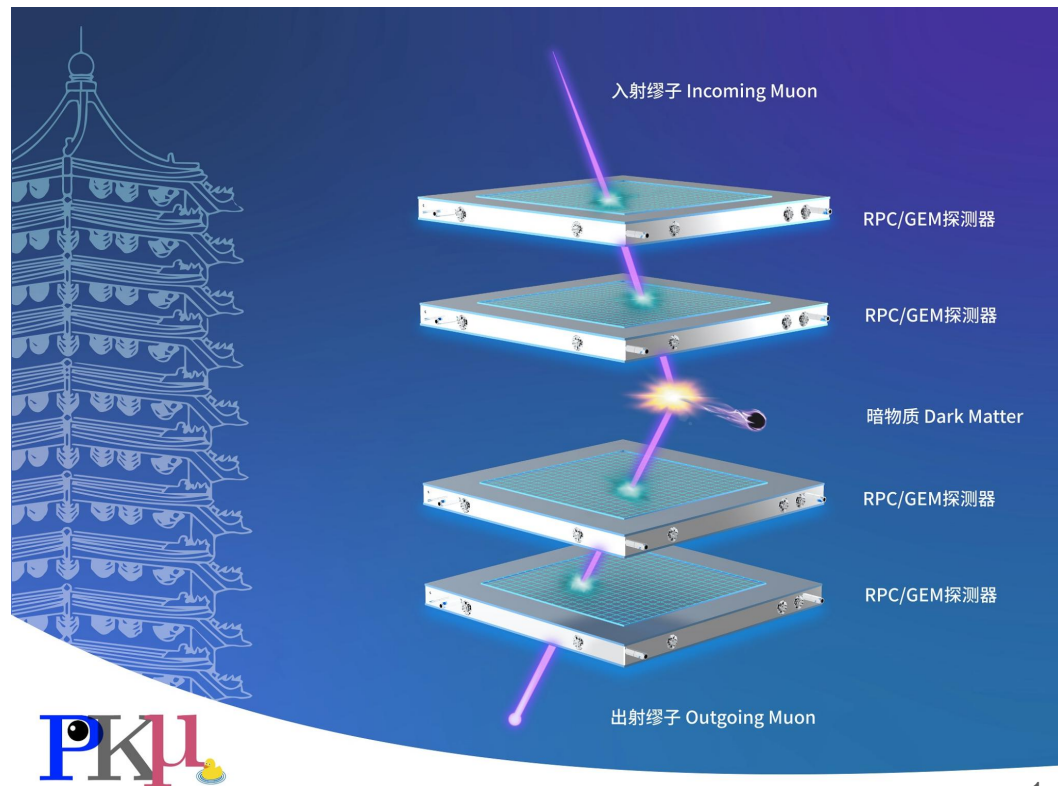
PKU-Muon Experiment for Muon Tomography and Exotic Physics Search

Qiang Li, Qite Li,
Chen Zhou, Leyun Gao

**On behalf of
the PKMu Group**

MEPA 2024, Yunnan
2024/08/26

[Phys.Rev.D 110 \(2024\) 1, 016017](https://arxiv.org/abs/2408.01601)
<https://lyazj.github.io/pkmuon-site/categories/activities/>



PKU Muon Detector Development



- CMS Muon Trigger RPC: assembled and tested at PKU in around 2002
- RPC R&D for nuclear physics
- CMS GEM upgrade program



北大基地生产的第一个CMS GEM模块



CMS端盖缪子探测器 GEM升级

北京大学、清华大学、中山大学、北京航空航天大学

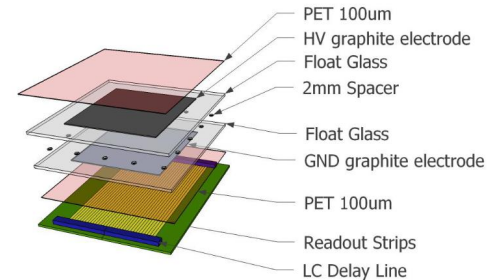
Combination of glass RPC & Delay-line Readout



Study of spatial resolution properties of a glass RPC
Qte Li, Yanlin Ye*, Chao Wen, Wei Ji, Yushou Song, Rongrong Ma, Chen Zhou, Yucheng Ge, Hongtao Liu
School of Physics and State Key Laboratory of Nuclear Physics and Technology, Peking University, Beijing 100871, China

Reference:

- 许金艳, 李奇特*, 等, *物理实验*, 41(2021)23
- Qi-Te, Li, et al. *Chinese Physics C* 37 (2013)016002.
- S. Chen, Q. Li*, et al, *JINST*: 10 (2014)10022.



90% R134a+9% i-C4H10+1% SF6 50ml/Min

Workshop on Muon Physics at the Intensity and Precision Frontiers (MIP 2024)

19 Apr 2024, 02:00 → 22 Apr 2024, 12:20 Asia/Shanghai

Peking University

Chen Zhou (Peking University (CN)), Qiang Li (Peking University (CN)), Qite Li (Peking University)



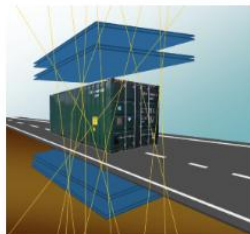
MIP2024

Several possible
Chinese Muon
beams in the near
future:
Melody,
CIADS, HIAF

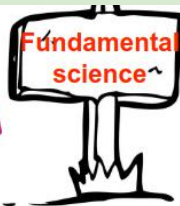
Muon: a bridge connecting applied and fundamental particle physics



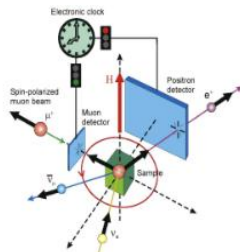
Void in Pyramid



Container inspection

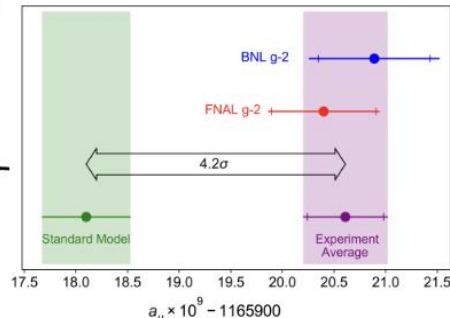


Bridge in Beijing



muSR

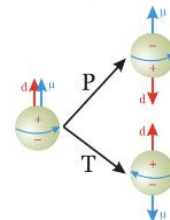
- Heavy fermion
- Superconductivity
- Quantum spin liquid
- ...



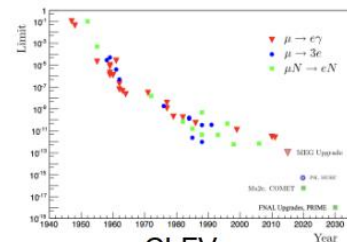
Muon g-2

Fundamental particle physics

- Muon g-2
- Muon EDM (Electric Dipole Moment)
- Muon CLFV (Charged Lepton Flavor Violation)
- Muon-philic DM (NA64 μ , MMM, this work)
- ...



EDM



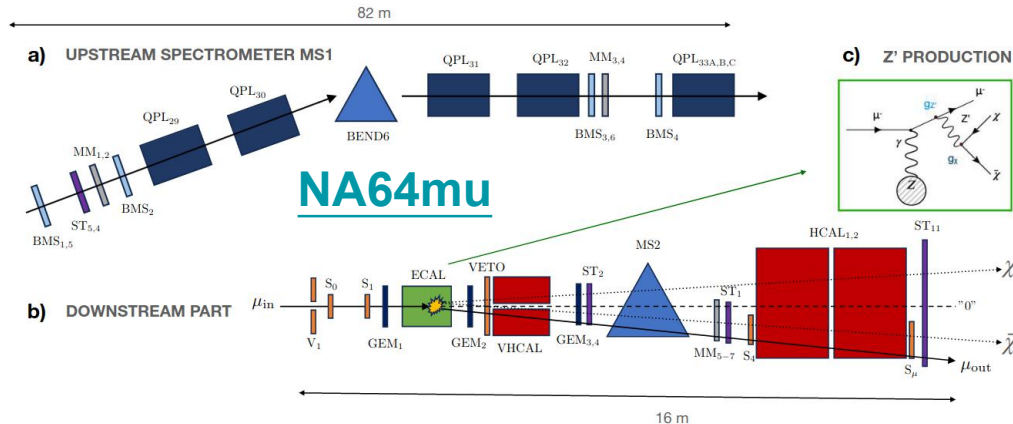
CLFV

Muongraphy: Non-destructive property!

- Geology:
 - Rock formations, glaciers, minerals, oceans and underground carbon dioxide storage*
- Archaeology:
 - pyramids in Egypt, Mausoleum of Qin Shihunag*
- Volcano monitor:
 - Showa-Shinzan, Asama, Sakurajima in Japan, and Stromboli in Italy*
- Tropic Cyclones monitor:
 - Kagoshima, Japan*
- Nuclear safety monitor:
 - Visualization of reactor interiors, detection of spent nuclear fuel in dry storage barrels and nuclear waste*
- ...

Muon Philic Dark Matter

- Muon Philic Dark Matter may be possible or necessary!
- Electron/Muons on Target Experiments
- DarkShine is ~ LDMX based on Shanghai Synchrotron Radiation Facility
- MMM (M3) is a US proposed muon-LDMX experiment
 - Intrigued by a proposal based on CERN NA64
 - “a lower-energy, e.g. 15 GeV, muon beam allows for greater muon track curvature and, therefore, a more compact experimental design...”



Light Dark Matter

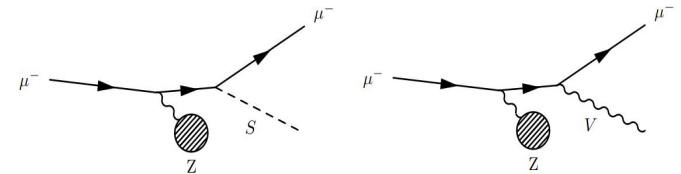


Figure 1. Dark bremsstrahlung signal process for simplified models with invisibly decaying scalar (*left*) and vector (*right*) forces that couple predominantly to muons. In both cases, a relativistic muon beam is incident on a fixed target and scatters coherently off a nucleus to produce the new particle as initial- or final-state radiation.

Exotic Dark Matter concentrated near the Earth

PHYSICAL REVIEW LETTERS 131, 011005 (2023)

Dark Matter Annihilation inside Large-Volume Neutrino Detectors

Owing to their interactions with ordinary matter, a strongly interacting dark matter component (DMC) would be trapped readily in the Earth and thermalize with the surrounding matter. Furthermore, for lighter DM, strong matter interactions allow Earth-bound DM particles to distribute more uniformly over the entire volume of the Earth rather than concentrating near the center. Together, this can make the DM density near the surface of the Earth tantalizingly large, up to $\sim f_\chi \times 10^{15} \text{ cm}^{-3}$ for DM mass of 1 GeV [8–11]. Despite their large surface abundance, such thermalized DMCs are almost impossible to detect in traditional direct detection experiments as they carry a minuscule amount of kinetic energy $\sim kT = 0.03 \text{ eV}$. A

- A large amount of dark matter is concentrated near the Earth, and their speed is very low, making it difficult to cause recoil signals in experiments. (大量暗物质集中在地球附近，它们的速度很低，很难在实验中引起足够的反冲信号)
- **As we will see, muon DM scattering experiment (PKMuon) depends minorly on DM velocity**

Muon Tomography and Muon-DM scattering

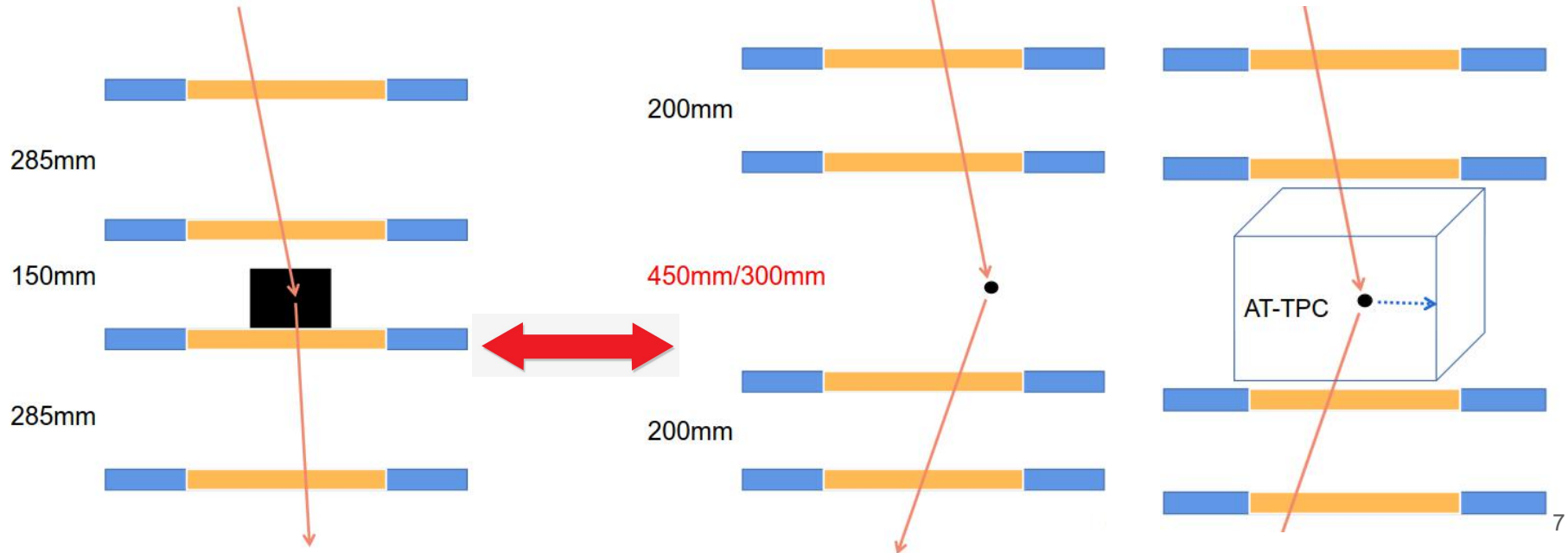
Muon Tomography

繆子成像

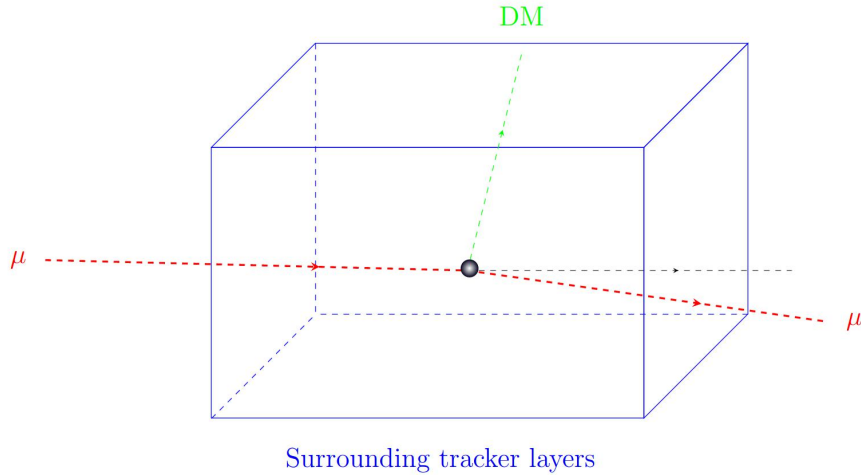
Dark Matter Search

暗物质寻找

[Phys.Rev.D 110 \(2024\) 1, 016017](#)



Muon DM Box experiment: qualitative estimation



Notice for high speed muons, it is appropriate to treat DM as frozen in the detector volume (V), and the estimated rate per second could be:

$$\rho V / M_D \times \sigma_D \times F_\mu,$$

The local density of DM is at the order of $\rho \sim 0.3$ GeV/cm³ and with a typical velocity of $v = 300$ km/s. While F_μ is the muon flux $\sim 1/60$ /s/cm² at the sea level. For Dark Matter mass $M_D \sim 0.1$ GeV, and detector box volume as $V \sim 1$ m³. Thus the sensitivity on Dark Matter Muon scattering cross section for 1 year run will be around

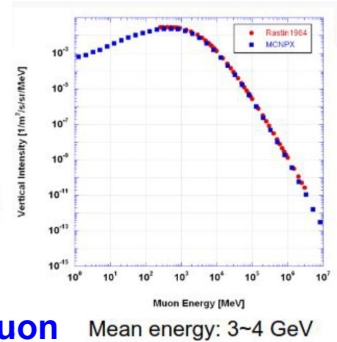
$$\sigma_D \sim 10^{-12} \text{ cm}^2$$

One year

Muon DM Box experiment: Geant4 Simulation

→ MC simulation of GEM-based detector based on **Geant4**

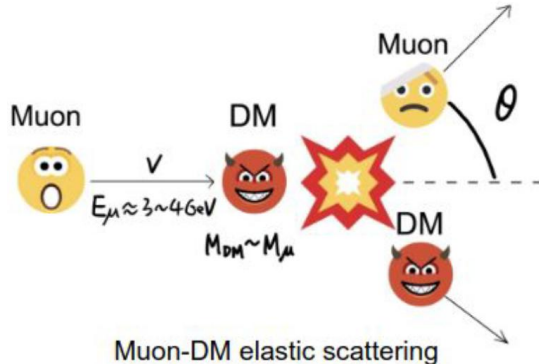
- ❖ Triple-GEM detector design refer to [CMS GEM design](#)
- ❖ Muon material interaction automatically considered by Geant4
- ❖ Reco hit position: Truth hit position smeared by GEM detector resolution (~ 200 um)



→ DM and muon scattering: **model-independent method**

Cosmic Muon Mean energy: 3~4 GeV

- ❖ Non-relativistic two-body elastic scattering between muon and DM following Newtonian mechanics
- ❖ Standard halo model: DM velocity distribution follows Maxwell-Boltzmann distribution
- ❖ [CRY](#) (Cosmic-ray) model: cosmic-ray muon energy and zenith angle distributions at sea-level



**Different from XENON1T/PandaX:
Relativistic muon hit quasi-static DM**

Muon DM Box experiment: Geant4 Simulation

Cos θ distribution in air has no obvious difference between that in a vacuum. Considering cost and technical difficulty, **vacuuming of the boxes is not necessary in Phase I of the project.**

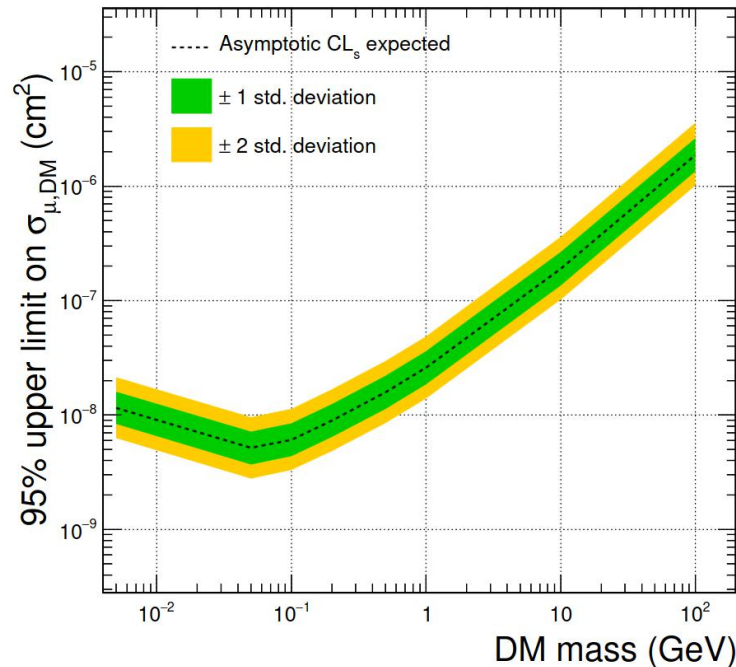
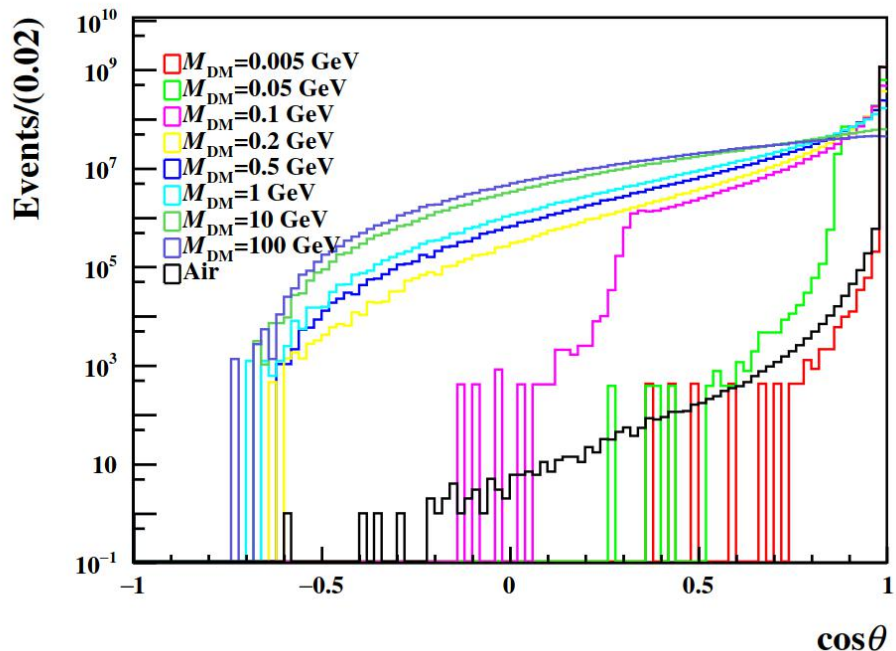
Cos θ distributions in Maxwell-Boltzmann velocity distribution and a constant velocity distribution are similar. Therefore, **our signal distribution and detection is not sensitive to the DM velocity model.**

As the DM mass increases, a larger fraction occupies the region of large scattering angles, resulting a more pronounced discrepancy between the signal and background.

Background	Event Number ($\times 10^9$)	
Air	1.15	
Vacuum	1.14	
DM mass (GeV)	Constant (%)	Maxwell-Boltzmann (%)
0.005	27.10 ± 0.01	27.11 ± 0.01
0.05	29.56 ± 0.01	29.55 ± 0.01
0.1	27.66 ± 0.01	27.64 ± 0.01
0.2	25.01 ± 0.01	24.99 ± 0.01
0.5	21.47 ± 0.01	21.46 ± 0.01
1	18.67 ± 0.01	18.66 ± 0.01
10	11.10 ± 0.01	11.10 ± 0.01
100	8.44 ± 0.01	8.43 ± 0.01

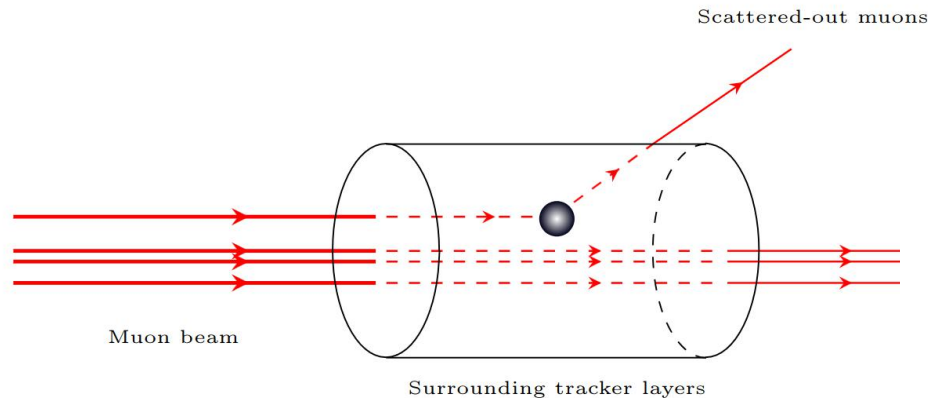
TABLE I. Background event numbers corresponding to the integrated luminosity of one-year exposure with the box filled with air and vacuum, along with the signal detection efficiency under different assumptions of DM velocity distribution and mass.

Muon DM Box experiment: expected results



- “Asimov” data is used
- Binned maximum likelihood fits
- UL determined by CLs method
- Only take statistical uncertainty into consideration

Muon DM Beam experiment: qualitative estimation



For $M_D = 0.03 \text{ GeV}$, $L = 1 \text{ m}$, and $N_\mu \sim 10^6/\text{s}$ (e.g., CSNS Melody design), and one year 10^7 s .

$$N = 10^{13} \times \sigma_D \times 100/\text{cm}^2,$$

Thus the sensitivity on Dark Matter Muon scattering cross section for 1 year run will be around

The estimated rate per second:

$$dN/dt = N_\mu \times \sigma_D \times L \times \rho/M_D,$$

$$\sigma_D \sim 10^{-15} \text{ cm}^2$$

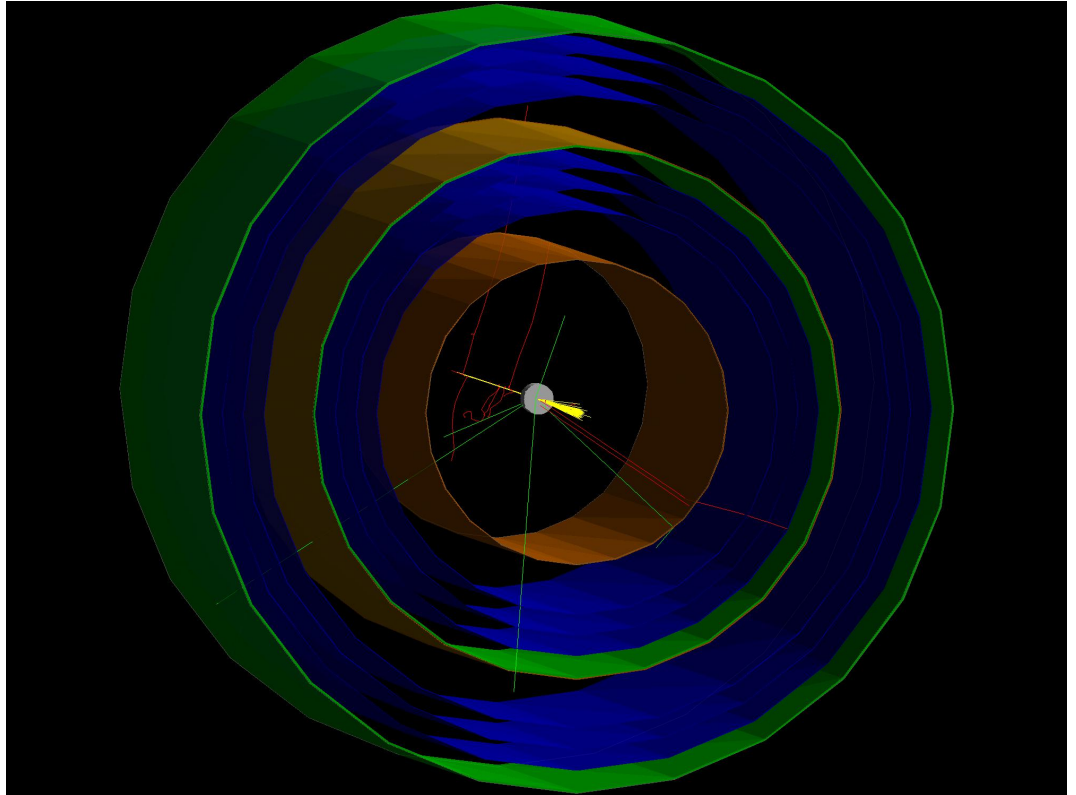
One year

Notice the surrounding area is around 100 cubic centimeters.

Muon DM Beam experiment: Geant4 Simulation

Simulating 1 GeV muon beam hit lead plate passing through GEM detector: the inner diameter of our CGEM detector is designed to be **50 mm**, which is **5 times the beam spot**.

Orange surfaces are drift cathodes. The blue surfaces are GEM foils. The green surfaces are PCBs. The yellow lines are muons tracks. The red curves are electron tracks. The green lines are photons.



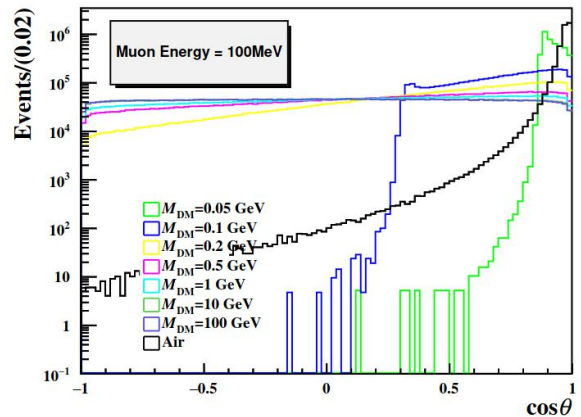
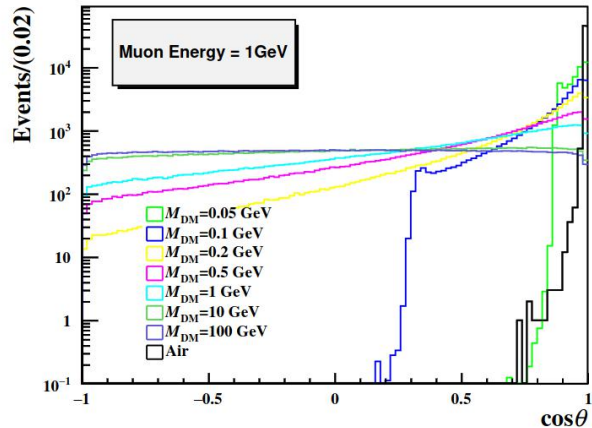
Cylindrical GEM (CGEM) detector structure for BESIII inner tracker system upgrade

Muon DM Beam experiment: Geant4 Simulation

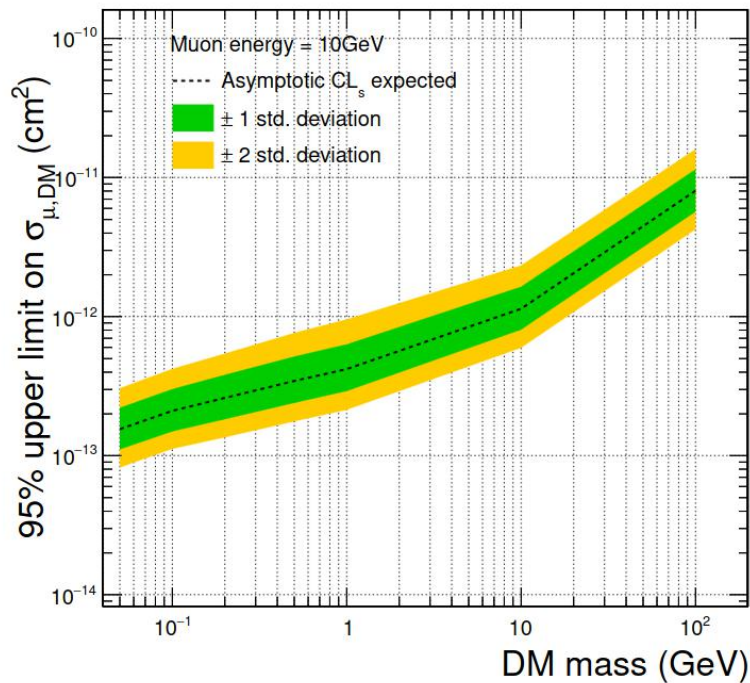
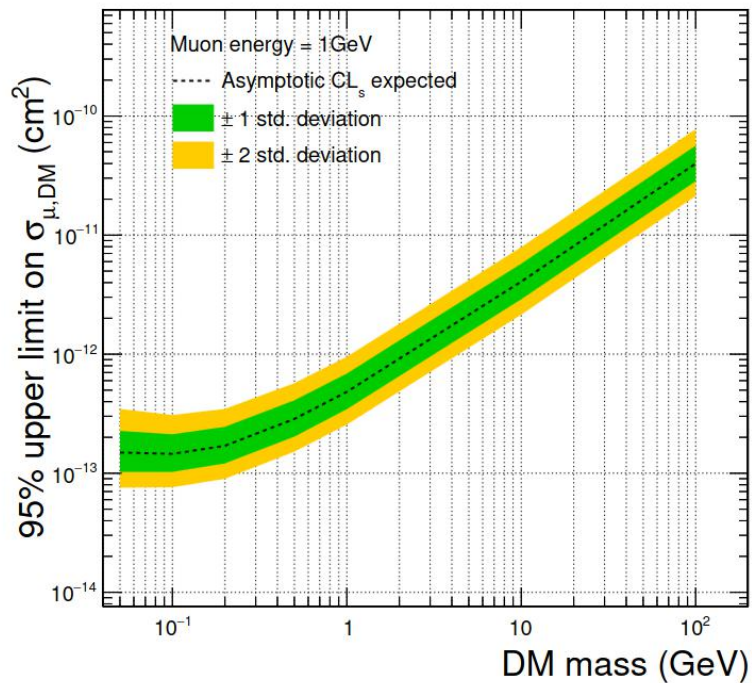
If the scattering angle is large enough, muons may hit the surrounding detector.

$M_{\text{DM}} \setminus E_{\text{kin}}^\mu$	100 MeV (%)	1 GeV (%)	10 GeV (%)
0.05 GeV	84.29 ± 0.04	74.85 ± 0.04	45.93 ± 0.05
0.1 GeV	91.74 ± 0.03	83.07 ± 0.04	58.17 ± 0.05
0.2 GeV	94.35 ± 0.02	88.16 ± 0.03	68.37 ± 0.05
0.5 GeV	95.17 ± 0.02	92.16 ± 0.03	78.91 ± 0.04
1 GeV	95.34 ± 0.02	93.88 ± 0.02	84.68 ± 0.04
10 GeV	95.35 ± 0.02	95.36 ± 0.02	94.06 ± 0.02
100 GeV	95.43 ± 0.02	95.37 ± 0.02	95.37 ± 0.02

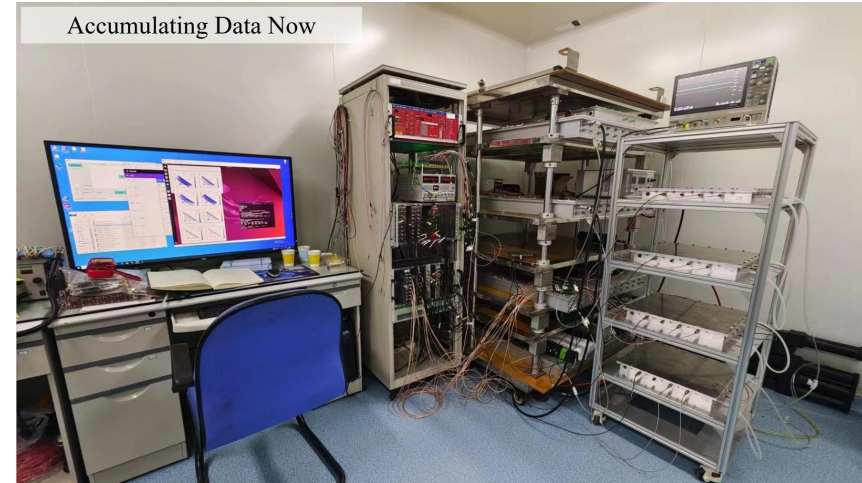
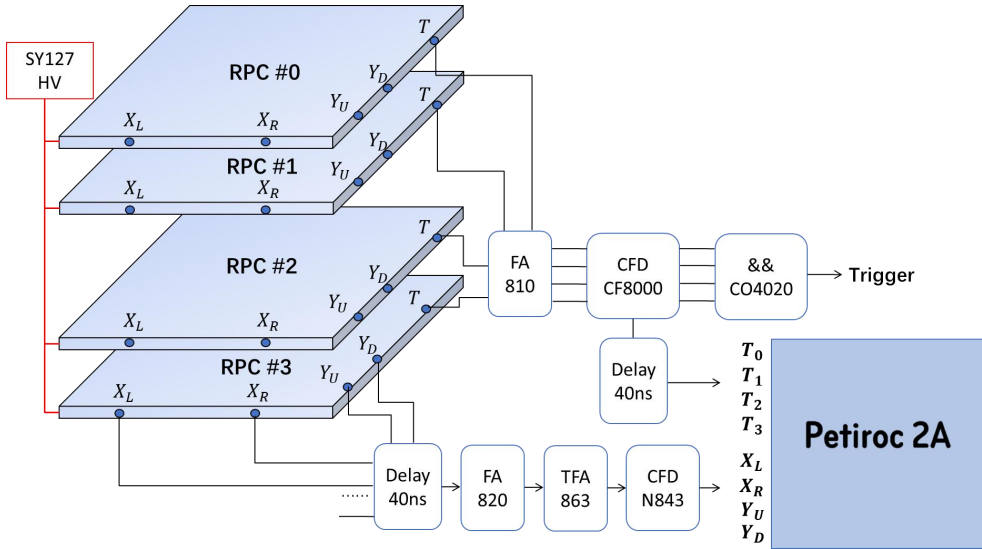
TABLE II. Signal detection efficiency under different assumptions of DM mass and muon beam energies.



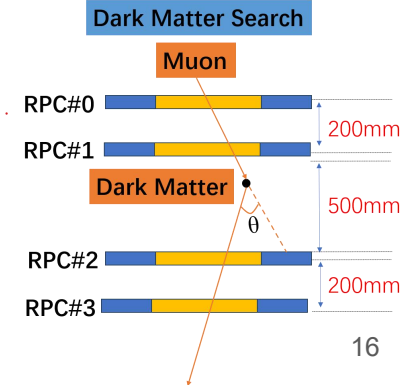
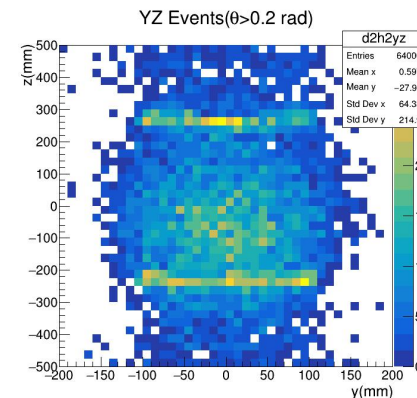
Muon DM Beam experiment: expected results



Current Box Exp. Status



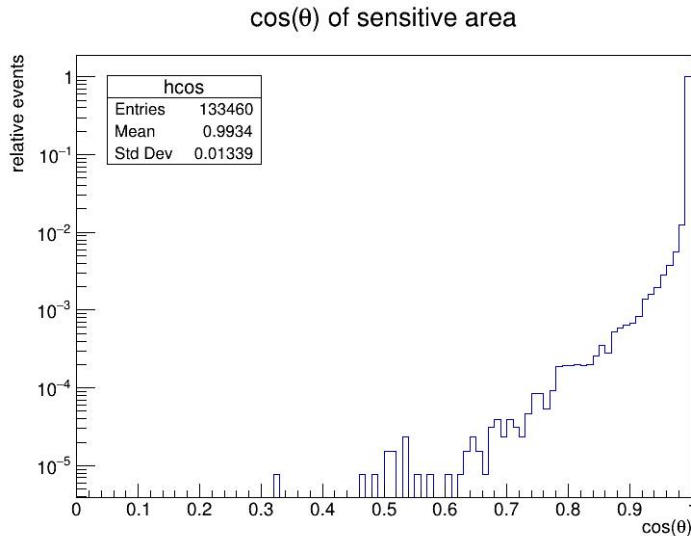
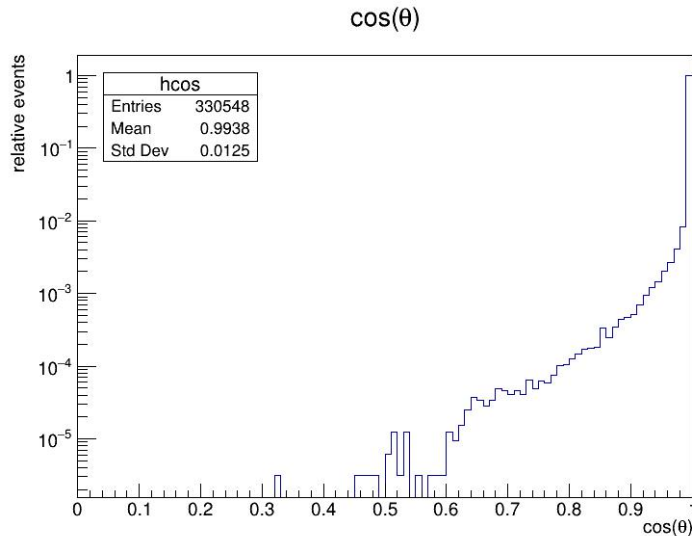
- data accumulated 3 month in air
- sensitive volume $50 \times 20 \times 20 \text{ cm}^3$
- 330548 valid events
- mean scattering angle 0.0252 rad
- 1.6% $\theta > 0.2 \text{ rad}$



Current Box Exp. Status

- $\theta > 0.2\text{rad}$ exists in sensitive area
 - 133460 valid events
 - 2999(2.247%) $\theta > 0.2\text{rad}$
 - mean scattering angle 0.0315rad

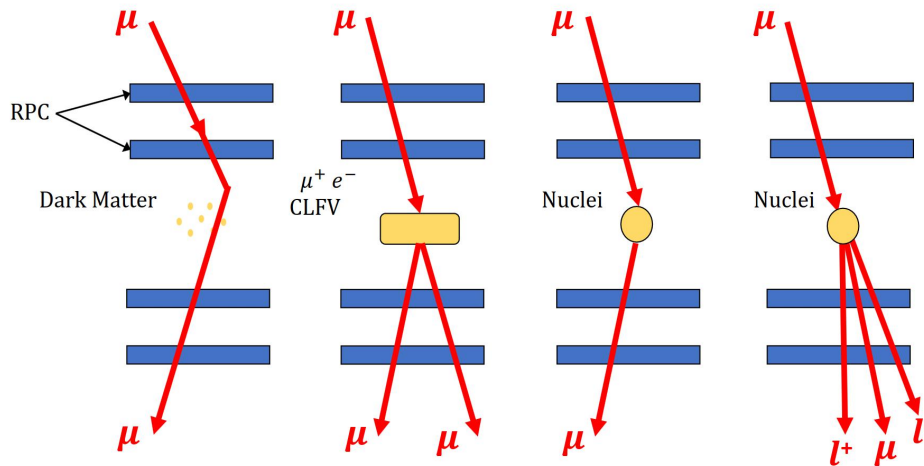
PRELIMINARY



Future

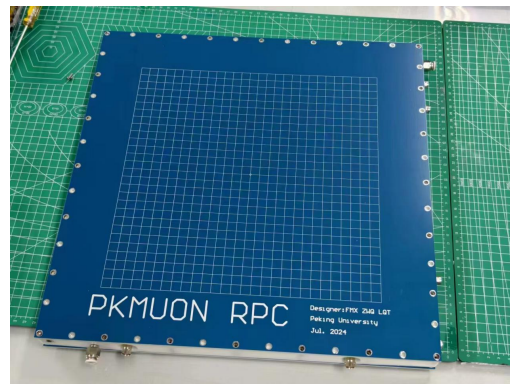
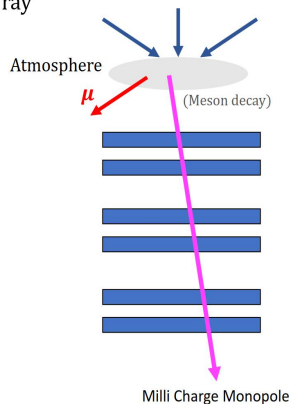
Interfacing Cosmic Muon or Muon beam

→Cosmic μ or μ beam



Telescope

→Cosmic ray

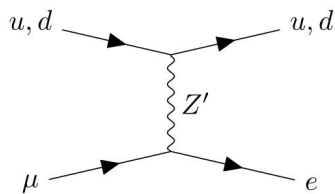


More physics program:
CLFV, Muon-Nuclei scattering ...

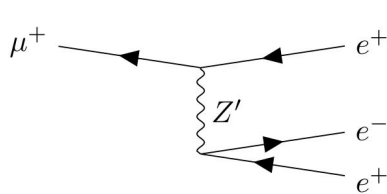
Larger area
RPC or GEM
being produced

Muon electron-target cLFV study

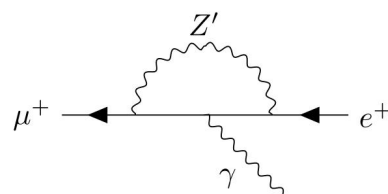
In the SM framework, the cLFV processes are strongly suppressed due to the tiny mass of neutrinos, hence unobservable in the current experiments yet. However, it may be much enhanced in various BSM models, such as **super-symmetry (SUSY)** [28], **leptoquark** [29], **two-Higgs-doublet** [36], **R-parity-violating (RPV) Minimal Super-symmetric Standard Model (MSSM)** [31–33], and the **heavy neutral gauge boson Z'** [30] studied in this paper. In the past decades, searches for the cLFV process were performed in different channels with several approaches, typically the high intensity muon-based experiments including **$\mu^+ \rightarrow e^+ \gamma$ (MEG)** [12], **$\mu^+ \rightarrow e^+ e^+ e^-$ (SINDRUM)** [13] and **$\mu^- N \rightarrow e^- N$ (SINDRUM II)** [14–17], as well as the **collider-based searches** for cLFV decays of Z [18–20], Higgs [21, 22] and several hadron resonances [8–10, 23]. Meanwhile, there will be continuous new experiments conducted in the near future to constantly improve the existing limits, such as **MEGII** [24], **Mu3e** [25], **COMET** [27] and **Mu2e** [26].



(a) $\mu - e$ conversion

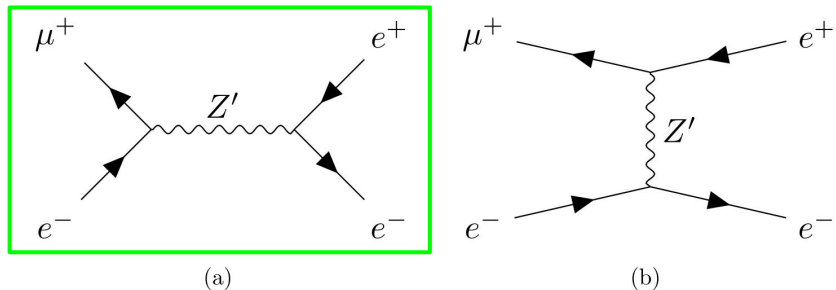


(b) $\mu^+ \rightarrow e^+ e^+ e^-$



(c) $\mu^+ \rightarrow e^+ \gamma$

Muon electron-target cLFV study

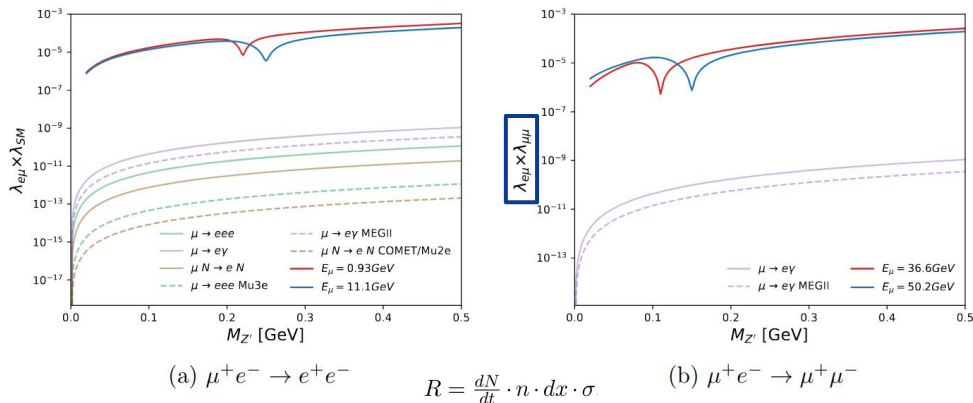


$$E_{cm} = \sqrt{2E_{\mu}m_e + m_{\mu}^2 + m_e^2}$$

Table 4: Resonant collision energy of process $\mu^+e^- \rightarrow e^+e^-$ and $\mu^+e^- \rightarrow \mu^+\mu^-$ with different $M_{Z'}$.

Process	$M_{Z'} / \text{GeV}$	E_{μ} / GeV	E_e / MeV	E_{cm} / GeV
$\mu^+e^- \rightarrow e^+e^-$	0.11	0.93	0.511	0.1101
	0.15	11.1	0.511	0.1501
	0.20	28.2	0.511	0.1996
$\mu^+e^- \rightarrow \mu^+\mu^-$	0.22	33.6	0.511	0.2200
	0.25	50.2	0.511	0.2499
	0.30	77.2	0.511	0.2998

Figure 2: The Feynman diagrams of the process $\mu^+e^- \rightarrow e^+e^-$: (a) s-channel and (b) t-channel.



$$R = \frac{dN}{dt} \cdot n \cdot dx \cdot \sigma$$

$$\Gamma(\mu \rightarrow e\gamma) = \frac{\alpha G_F^2 m_{\mu}^3 M_{Z'}^4}{4\pi^4 M_{Z'}^4} \left[\sin^2 \theta_W \left(\sin^2 \theta_W - \frac{1}{2} \right) \right]^2 (\lambda_{ee} \lambda_{e\mu} m_e + \lambda_{\mu\mu} m_{\mu})^2$$

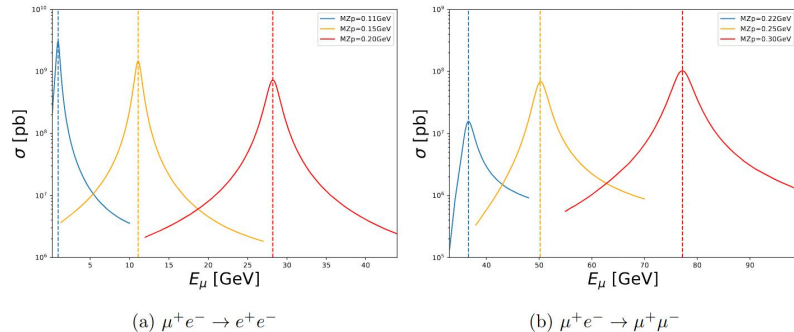
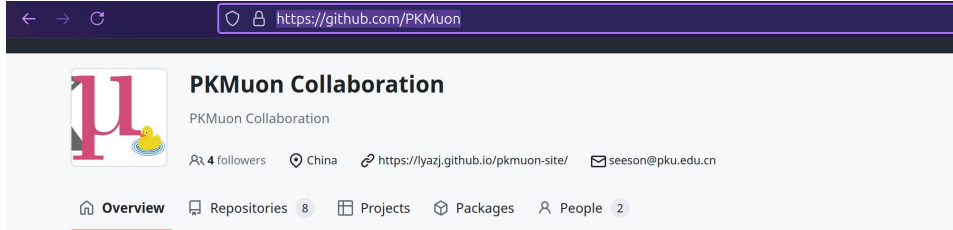


Figure 9: Cross section for resonant production of the process $\mu^+e^- \rightarrow e^+e^-$ and $\mu^+e^- \rightarrow \mu^+\mu^-$ with different $M_{Z'}$.

Growing PKMuon Software Framework

Collaborate on GitHub



PKMuon Collaboration

PKMuon Collaboration

4 followers China https://lyazi.github.io/pkmuon-site/ seeson@pku.edu.cn

Overview Repositories 8 Projects Packages People 2

Pinned

PKMUON_G4sim Public

Forked from yuxdPKU/PKMUON_G4sim

Geant4-based simulation of PKMUON

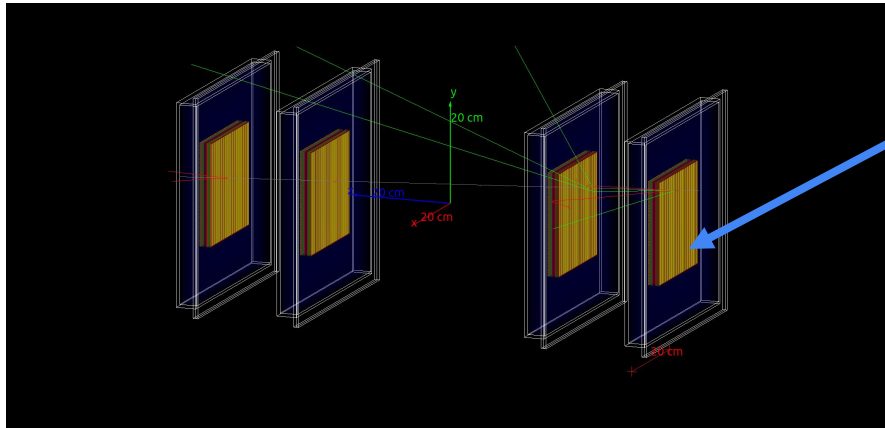
C++

geomu Public

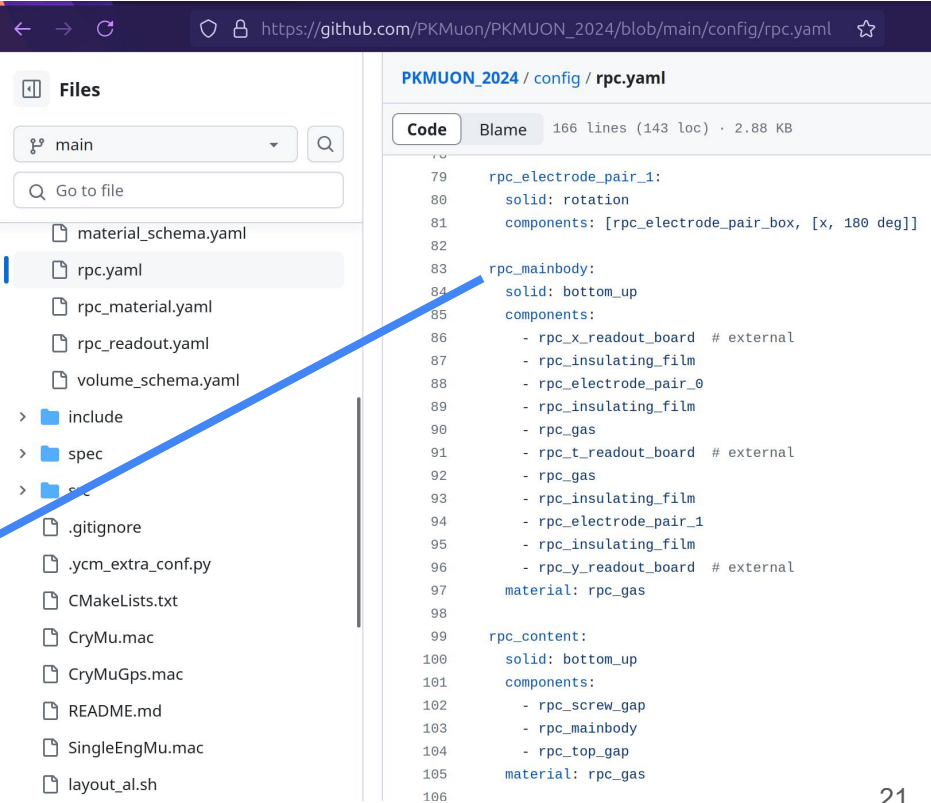
Forked from lyazi/geomu

Geographic Muon Simulation

C++



Organize geometry modularly and extensibly



Files

main

Go to file

- material_schema.yaml
- rpc.yaml
- rpc_material.yaml
- rpc_readout.yaml
- volume_schema.yaml
- include
- spec
- src
- .gitignore
- .ycm_extra_conf.py
- CMakeLists.txt
- CryMu.mac
- CryMuGps.mac
- README.md
- SingleEngMu.mac
- layout_al.sh

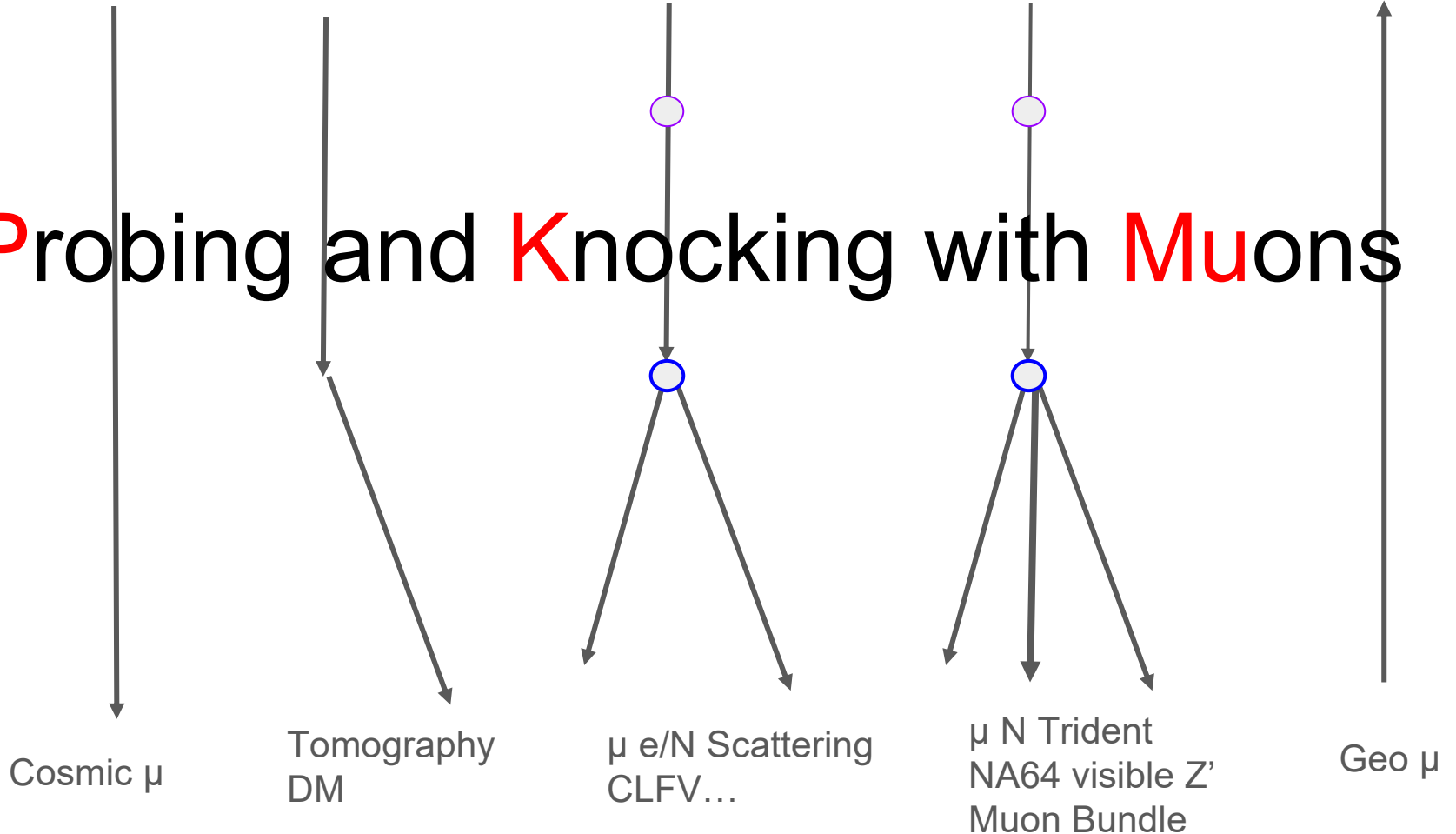
PKMUON_2024 / config / rpc.yaml

Code Blame 166 lines (143 loc) · 2.88 KB

```
79 rpc_electrode_pair_1:
80   solid: rotation
81   components: [rpc_electrode_pair_box, [x, 180 deg]]
82
83 rpc_mainbody:
84   solid: bottom_up
85   components:
86     - rpc_x_readout_board # external
87     - rpc_insulating_film
88     - rpc_electrode_pair_0
89     - rpc_insulating_film
90     - rpc_gas
91     - rpc_t_readout_board # external
92     - rpc_gas
93     - rpc_insulating_film
94     - rpc_electrode_pair_1
95     - rpc_insulating_film
96     - rpc_y_readout_board # external
97   material: rpc_gas
98
99 rpc_content:
100  solid: bottom_up
101  components:
102    - rpc_screw_gap
103    - rpc_mainbody
104    - rpc_top_gap
105  material: rpc_gas
106
```

Backup

Probing and Knocking with Muons



Melody, CIADS, HIAF Muon beams

Melody: approved and the first Chinese Muon beam will be built in 5 years.

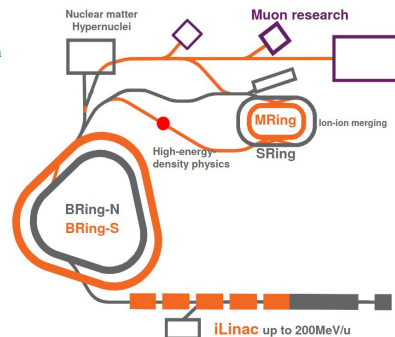
	Surface Muon	Negative Muon	Decay Muon
Proton Power (kW)	20	Up to 100	Up to 100
Pulse width (ns)	130 to 10	500	130 to 10
Muon intensity (/s)	$10^5 \sim 10^6$	Up to 5×10^6	Up to 5×10^6
Polarization (%)	>95	>95	50~95
Positron (%)	<1%	NA	<1%
Repetition (Hz)	1	Up to 5	Up to 5
Terminals	2	1~2	2
Muon Momentum (MeV/c)	30	30	Up to 120
Full Beam Spot (mm)	10 ~ 30	10 ~ 30	10~30

HIAF & HIAF-U



- **BRing-N**: 34Tm, 569m, 3Hz
- **SRing**: 17(25)Tm, 270.5m, accumulation/compression
- **BRing-S**: 86Tm, 3Hz, superconducting
- **MRing**: 45Tm, superconducting, beam merging

	Particle (GeV/u)	Intensity (ppp)	Est. time
FAIR	2.7	$^{238}\text{U}^{28+}$ 5×10^{11}	2025
NICA	4.5	$^{197}\text{Au}^{32+}$ 4×10^9	2022
FNAL	8.0	p 6.8×10^{13}	2028
	3.0	$^{238}\text{U}^{35+}$ 2×10^{12}	
HIAF-U	9.1	$^{238}\text{U}^{92+}$ 1×10^{12}	2032
	25	p 4×10^{14}	



~30 MeV, ~100 MeV,

~1GeV

PoCA

- The point of closest approach (PoCA) algorithm
- The angular scattering distribution is approximately Gaussian

$$\sigma_{\theta} = \frac{13.6 \text{ MeV}}{\beta c p} \sqrt{\frac{L}{L_0}} \left[1 + 0.038 \ln \frac{L}{L_{\text{rad}}} \right] \approx \frac{13.6}{p} \sqrt{\frac{L}{L_0}}$$

❖ p : momentum, βc : velocity, L : depth of the material, L_{rad} : radiation length of the material

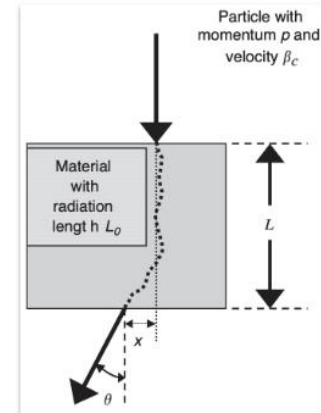
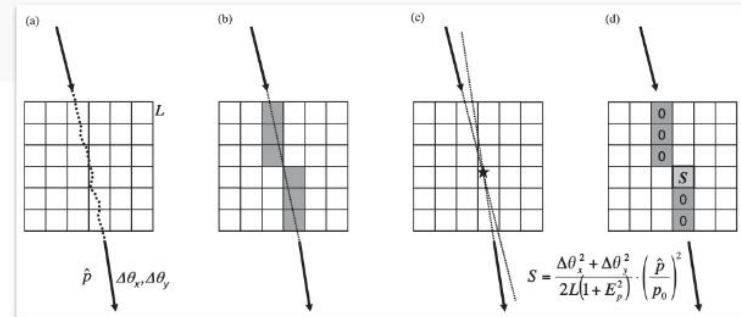
- Scattering strength: establish a nominal muon momentum (3 GeV, for example), and define the mean square scattering of nominal muons per unit depth of a material

$$\lambda_{\text{mat}} = \left(\frac{13.6}{p_0} \right)^2 \frac{1}{L_{\text{rad}}} \approx \sigma_{\theta_0, \text{mat}}^2$$

❖ depends only on material radiation length, and varies strongly with material Z

- Multiple muons income and scatter with material, and we measure it in two orthogonal planes x and y . If we know the path length L_i and the momentum p_i of each muon through the material:

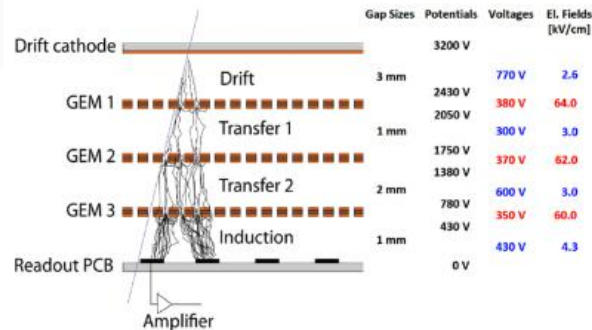
$$\hat{\lambda} = \frac{1}{N} \sum_{i=1}^N N \left(\frac{p_i^2}{p_0^2} \cdot \frac{\theta_{xi}^2 + \theta_{yi}^2}{2L_i} \right)$$



→ Triple-GEM detector installed in the CMS experiment

- ❖ Improve trigger capabilities and muon measurements
- ❖ Excellent performance: rate $> 10 \text{ kHz/cm}^2$, time resolution $\sim 8 \text{ ns}$, spatial resolution $\sim 200 \mu\text{m}$

CMS TDR

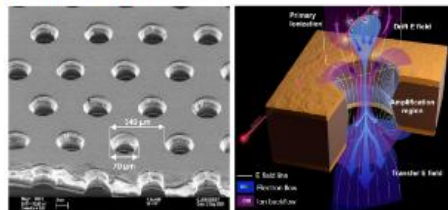


Schematic view of a triple-GEM detector

→ Electron amplification structure and flexible readout structures

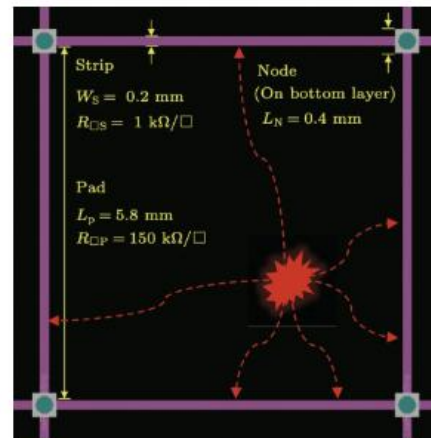
→ Pixel readout VS resistive anode readout method

- ❖ Challenge: Large amount of small pixels
- ❖ Good comparable spatial resolution but less electronic channels



→ Design our exclusive readout for the specific requirements of PKU-Muon GEM detectors.

- ❖ Hit position reconstruction algorithm ongoing



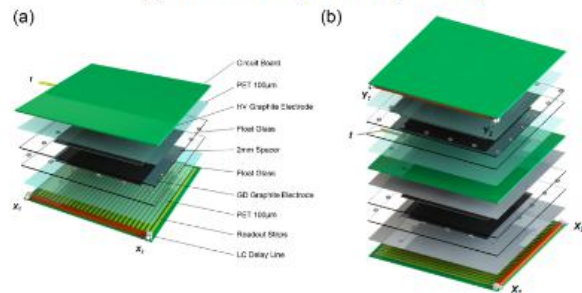
Structure diagram of the basic resistive anode cell

RPC

Compact Muon Solenoid



(a) Prototype glass RPC
(b) One RPC with two structure get X and Y signals respectively



→ RPC — R. Santonico (in 1980s)

- ❖ simple and robust structure, long-term stability, good timing resolution, easy-maintenance and low cost

→ PKU RPC R&D History

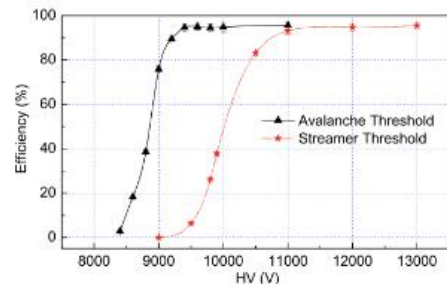
- ❖ **CMS Muon Trigger RPCs**, assembled and tested by PKU (2002)
- ❖ Combination of glass RPC & Decay-line Readout ([Qite Li et. al.](#))

→ Glass RPC MT Prototype in 2012

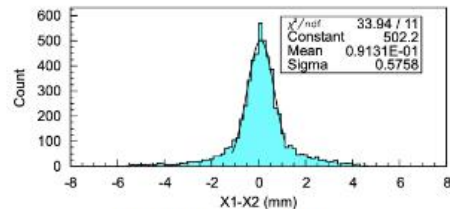
- ❖ Effective area of the electrode: $20 \times 20 \text{ cm}^2$
- ❖ Readout electronics: decay-line, charge-division methods

→ Good and stable performance so far!

- ❖ Positional resolution: $\sim 0.5 \text{ mm}$, detection efficiency: $> 90\%$



Efficiency curves for the glass RPC



Distribution of X1-X2

- A new species χ that interacts “strongly” with ordinary matter but that makes up only a tiny fraction $f_\chi = \rho_\chi / \rho_{\text{DM}} \ll 1$ of the total DM mass density
 - ❖ Be slowed significantly by scattering with matter in the atmosphere or the Earth before reaching the target, leading to energy depositions in the detector that are too small to be observed with standard methods
 - ❖ Be trapped readily in the Earth and thermalize with the surrounding matter.
 - ❖ For lighter DM, strong matter interactions allow Earth-bound DM particles to distribute more uniformly over the entire volume of the Earth rather than concentrating near the center.
- Make the DM density near the surface of the Earth tantalizingly large, up to $\sim f_\chi \times 10^{15} \text{ cm}^{-3}$ for DM mass of 1 GeV
 - ❖ Ordinary DM density $\sim 0.3 \text{ cm}^{-3}$
- Almost impossible to detect in traditional direct detection experiments as they carry a minuscule amount of kinetic energy $\sim kT = 0.03 \text{ eV}$

Exotic DM is slowed down near the Earth, and its density is highly enhanced

MMM

→ Motivated by $(g - 2)_\mu$ anomaly

→ M^3 (Muon Missing Momentum) based at Fermilab ([LINK](#))

❖ New fixed-target, missing-momentum search strategy to probe invisibly decaying particles that couple preferentially to muons

→ Advantage:

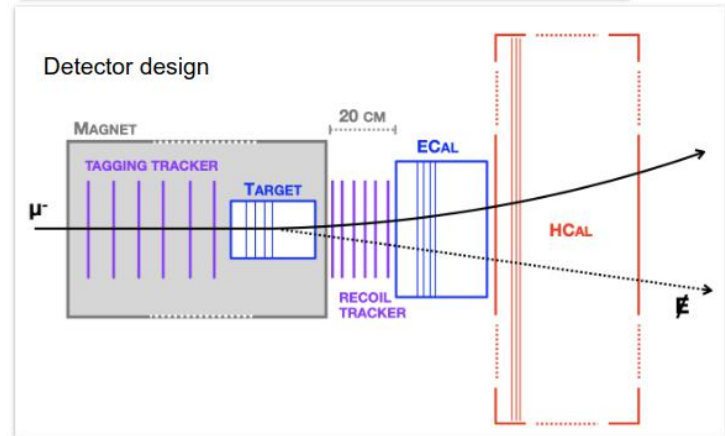
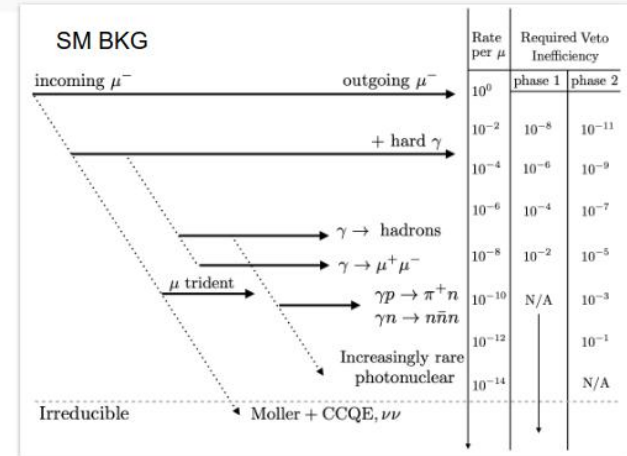
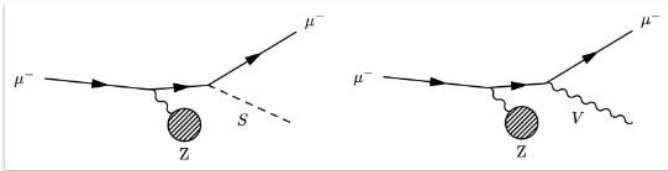
❖ Bremsstrahlung backgrounds suppressed

▸ Bremsstrahlung rate is suppressed by $(m_e/m_\mu)^2 \approx 2 \times 10^{-5}$

❖ Compact experimental design

▸ Lower muon beam energy (15 GeV vs. 100-200 GeV) allows for greater muon track curvature and more compact design

→ SM-induced BKG are studied



NA64 μ

→ $Z' U(1)_{L_\mu - L_\tau}$ model

- ❖ Z' directly couples the second and third lepton generations
- ❖ The extension model: interactions with DM candidates

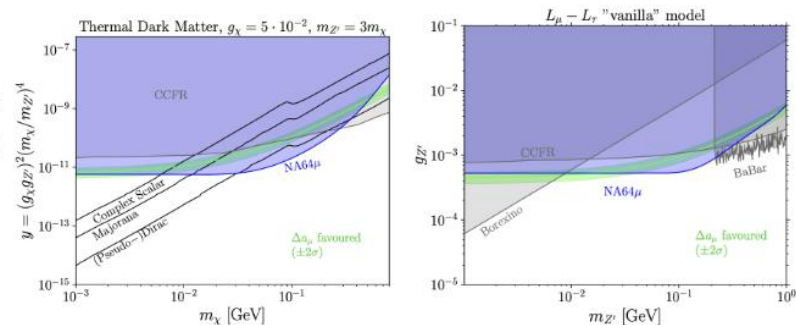
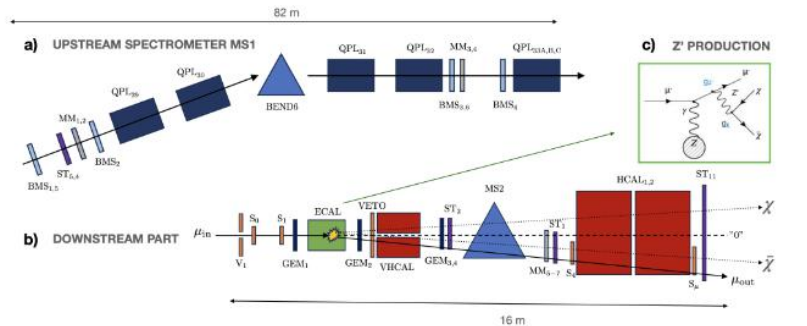
→ M2 beamline at the CERN Super Proton Synchrotron

- ❖ Incoming muon momentum 160 GeV/c
- ❖ Total accumulated statistics: $(1.98 \pm 0.02) \times 10^{10}$ MOT

→ Signal process: $\mu N \rightarrow \mu N Z', Z' \rightarrow$ invisible

→ No event falling within the expected signal region is observed

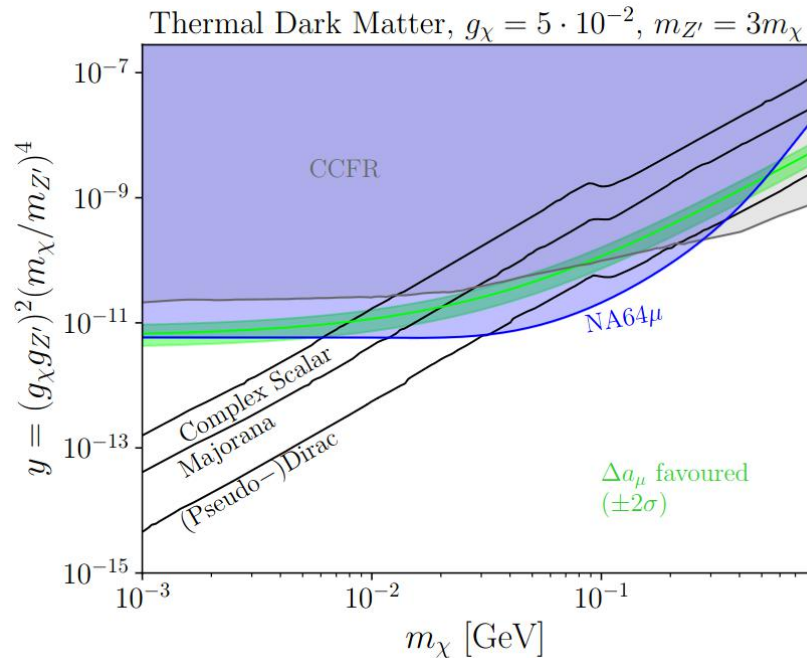
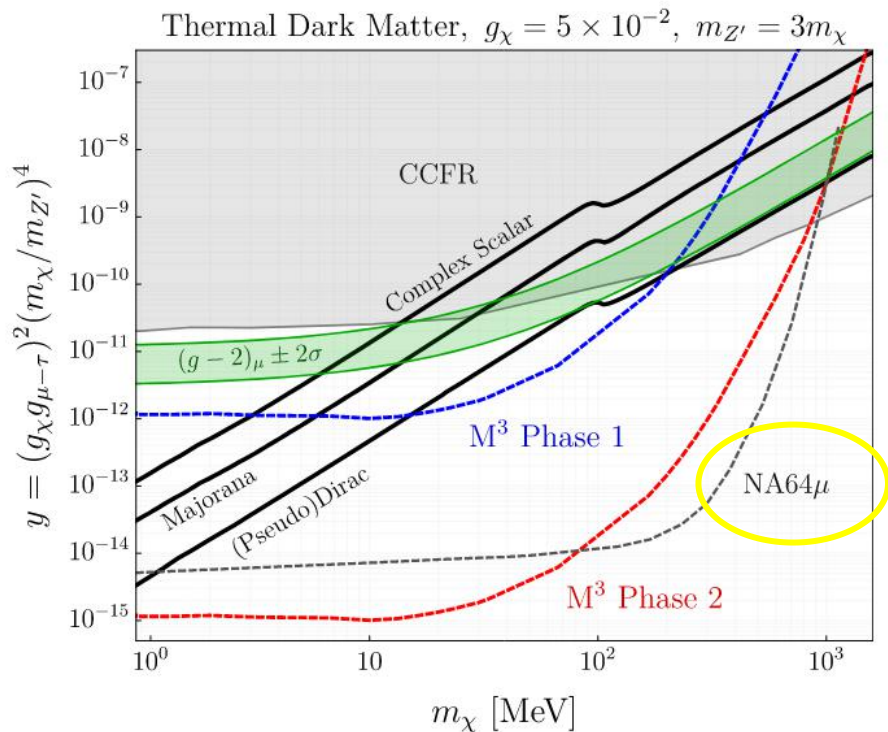
- ❖ 90% CL upper limits are set in the $(m_{Z'}, g_{Z'})$ parameter space of the $L_\mu - L_\tau$ vanilla model, constraining viable mass values for the explanation of $(g - 2)_\mu$ anomaly to $6 - 7 \text{ MeV} < m_{Z'} < 40 \text{ MeV}$, with $g_{Z'} < 6 \times 10^{-4}$.
- ❖ New constraints on light thermal DM for values $y > 6 \times 10^{-12}$ for $m_\chi > 40 \text{ MeV}$



Ref: [MMM](#)

VS

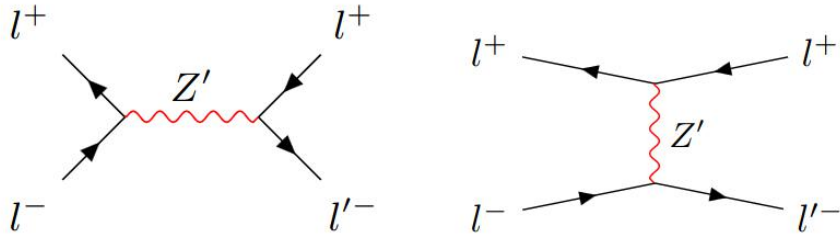
Ref: [NA64mu](#)



Muon-Electron Threshold Scan

Muon-electron collider

CLFV



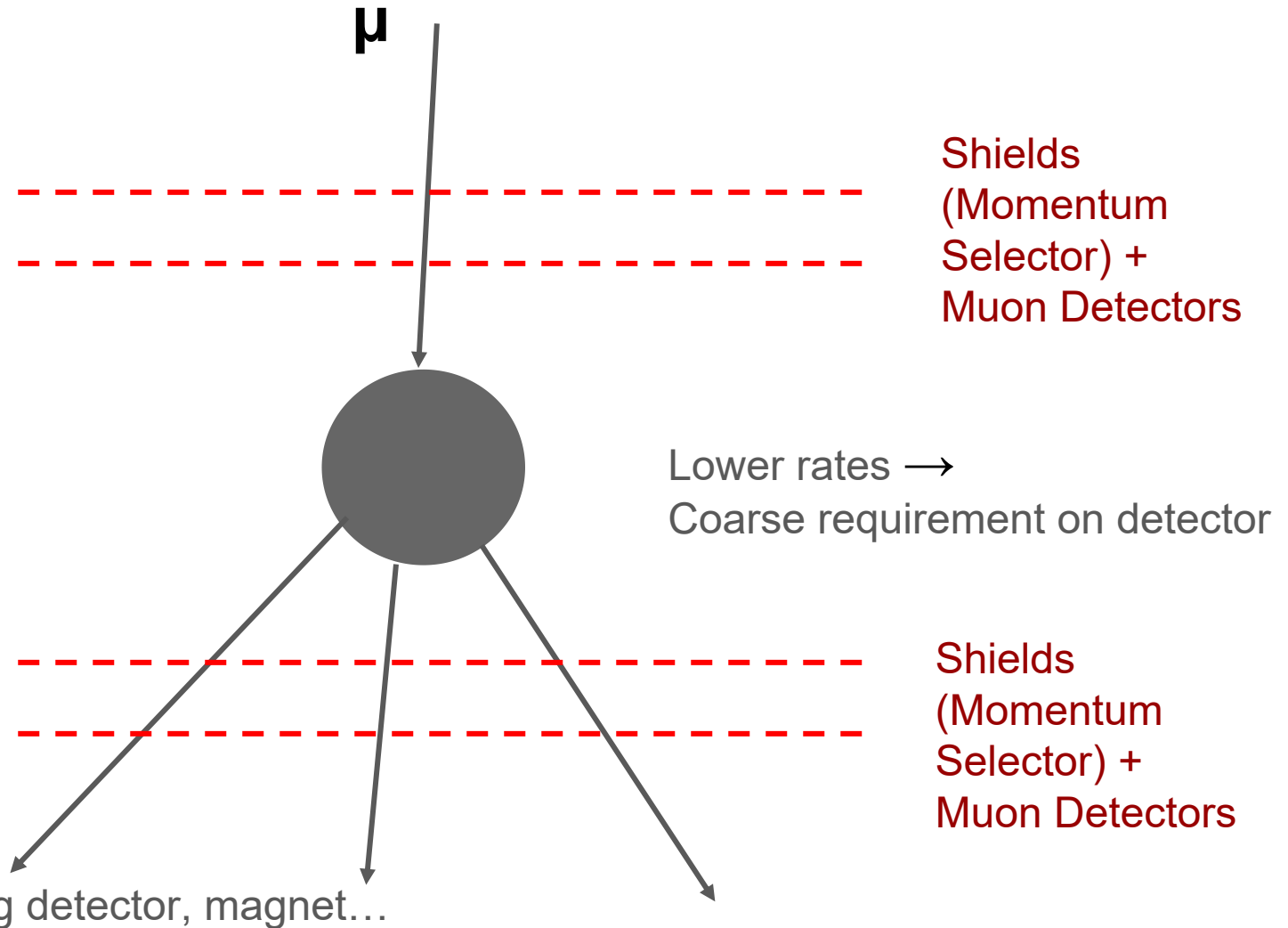
Muon-on-target

Process	$M_{Z'}$ / GeV	E_μ / GeV	E_e / MeV	E_{cm} / GeV
$\mu^+e^- \rightarrow e^+e^-$	0.11	0.93	0.511	0.1101
	0.15	11.1	0.511	0.1501
	0.20	28.2	0.511	0.1996
$\mu^+e^- \rightarrow \mu^+\mu^-$	0.22	33.6	0.511	0.2200
	0.25	50.2	0.511	0.2499
	0.30	77.2	0.511	0.2998

- $\mu^+ e^- \rightarrow Z' \rightarrow e^+ e^-$, $\mu^+ \mu^-$ Charged Lepton Flavor Violation
- $\mu^+ e^- \rightarrow Z' \rightarrow X X$ Lepton Flavor Violation DM
- Resonant production Enhancement
- [X=16.7 MeV Anomaly](#)
- Connecting e-mu collider and muon beam experiments

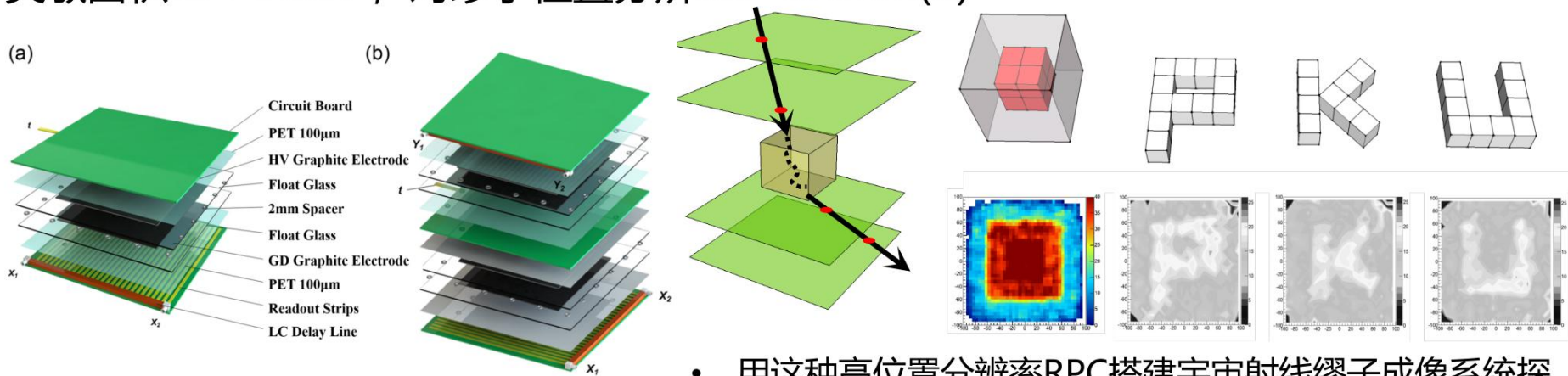
specific beam energy
Leads to
specific phase space

Cosmic Muon Collider



探测系统——高位置分辨率阻性板气体室(RPC)

- 首创大面积玻璃RPC与延迟块读出技术结合
- 灵敏面积 $20 * 20\text{cm}^2$ ，对缪子位置分辨 $0.3\sim 0.4\text{mm}(\sigma)$



参考文献:

- **Li, Qite**, et al. *NIM-A* 663.1 (2012): 22-25.
- **Qi-Te, Li**, et al. *Chinese Physics C* 37 (2013)016002.
- **S. Chen, Q.Li***, et al, *JINST*: 10 (2014)10022.
- 许金艳, 李奇特*, 等, *物理实验*, 41(2021)23

- 用这种高位置分辨率RPC搭建宇宙射线缪子成像系统探测宇宙射线缪子入射与出射径迹矢量，可测量到非常小的散射偏转角 $< 0.5\text{mrad}(0.3^\circ)$ ，重建灵敏区内物质分布信息
- 右图是北京大学缪子成像原型机对包裹在 $12 * 12 * 12\text{cm}^3$ 铁壳中的 $6 * 6 * 6\text{cm}^3$ 方形铅块，以及用 $3 * 3 * 3\text{cm}^3$ 铁块组成的PKU字母的成像结果

Preliminary experiment-simulation comparison

